



HAL
open science

A combination of cyclophosphamide and interleukin-2 allows CD4+ T cells converted to Tregs to control scurfy syndrome

Marianne Delville, Florence Bellier, Juliette Leon, Roman Klifa, Sabrina Lizot, H el ene Vin on, Steicy Sobrino, Romane Thouenon, Armance Marchal, Alexandrine Garrigue, et al.

► To cite this version:

Marianne Delville, Florence Bellier, Juliette Leon, Roman Klifa, Sabrina Lizot, et al.. A combination of cyclophosphamide and interleukin-2 allows CD4+ T cells converted to Tregs to control scurfy syndrome. *Blood*, 2021, 137 (17), pp.2326-2336. 10.1182/blood.2020009187 . hal-03588460

HAL Id: hal-03588460

<https://hal.science/hal-03588460v1>

Submitted on 9 May 2023

HAL is a multi-disciplinary open access archive for the deposit and dissemination of scientific research documents, whether they are published or not. The documents may come from teaching and research institutions in France or abroad, or from public or private research centers.

L'archive ouverte pluridisciplinaire **HAL**, est destin ee au d ep ot et  a la diffusion de documents scientifiques de niveau recherche, publi es ou non,  emanant des  tablissements d'enseignement et de recherche fran ais ou  trangers, des laboratoires publics ou priv es.



Distributed under a Creative Commons Attribution - NonCommercial 4.0 International License

A combination of cyclophosphamide, interleukin-2 allow CD4⁺ T cells converted to Tregs to control *scurfy* syndrome

Short title FOXP3 gene therapy to control IPEX syndrome

Marianne Delville^{1,2,3}, Florence Bellier¹, Juliette Leon^{1,4}, Roman Klifa^{1,5}, Sabrina Lizot¹, H el ene Vin on¹, Steicy Sobrino¹, Romane Thouennon¹, Armance Marchal¹, Alexandrine Guarrigue¹, Juliette Olivr e¹, So li Charbonnier¹, Chantal Lagresle-Peyrou^{1,3}, Mario Amendola, Axel Schambach, David Gross, Baptiste Lamarth e¹, Christophe Benoit⁴, Julien Zuber^{1,9}, Isabelle Andr e^{*1}, Marina Cavazzana^{*1,2}, Emmanuelle Six^{*1}

*These authors contributed equally to this work.

Affiliations

1. Universit e de Paris, Institut Imagine, INSERM, U1163, Paris, France
2. Service de Bioth rapie et d'Aph r ese, Groupe Hospitalier Universitaire Ouest, APHP, Paris, France
3. Centre d'investigation clinique Bioth rapie, Groupe Hospitalier Universitaire Ouest, APHP, Paris, France
4. Department of Immunology, Harvard Medical School, Boston, MA 02115, USA
5. Service d'Immuno-h matologie p diatrique, H pital Necker, APHP, Paris, France
6. Genethon, 91000, Evry, France
7. Institute of Experimental Hematology, Hannover Medical School, Hanover, Germany
8. Universit e de Paris, Institut Necker Enfants-Malades, INSERM, U1151, Paris, France.
9. Service de N phrologie et Transplantation r nale, H pital Necker, APHP, Paris, France

Corresponding author

Dr Marianne Delville

H pital Necker Enfant Malades

149, rue de S vres

75015 Paris

marianne.delville@aphp.fr

Tel +33 (0) 44 49 52 74

Fax +33 (0) 44 49 52 76

Key points

- Combination of a conditioning by cyclophosphamide and IL-2 allows suppressive T cells to rescue *scurfy* mice after disease onset
- Transcriptomic analysis reveals a lasting restoration of Treg identity in FOXP3-transduced *scurfy* cells – even an inflammatory environment

Abstract

Immunodysregulation polyendocrinopathy enteropathy X-linked (IPEX) syndrome is caused by mutations in *FOXP3*, which lead to the loss of function of regulatory T cells (Treg) and the development of autoimmune manifestations early in life. The selective induction of a Treg program in autologous CD4⁺ T cells by *FOXP3* gene transfer is a promising approach for curing IPEX. We have established a novel *in vivo* assay of Treg functionality, based on adoptive transfer of these cells into *scurfy* mice (an animal model of IPEX) and a combination of cyclophosphamide conditioning and interleukin-2 treatment. This model highlighted the possibility of rescuing *scurfy* disease after the latter's onset. By using this *in vivo* model and an optimized lentiviral vector expressing human Foxp3 and as a reporter a truncated form of the 5 low-affinity nerve growth factor receptor (Δ LNGFR), we demonstrated that the adoptive transfer of FOXP3-transduced *scurfy* CD4⁺ T cells enabled the long-term rescue of *scurfy* autoimmune disease. The efficiency was similar to that seen with wild-type Treg. After *in vivo* expansion, the converted CD4^{FOXP3} cells recapitulated the transcriptomic core signature for Treg. These findings demonstrate that FOXP3 expression converts CD4⁺ T cells into functional Treg capable of controlling severe autoimmune disease.

Keywords

regulatory T cell, gene therapy, *scurfy*, autoimmunity, IPEX, FoxP3

Abbreviation

7-AAD	7-aminoactinomycin D
ANOVA	analysis of variance
Anti-CD3	anti-CD3 Fab'2
CFSE	carboxyfluorescein succinimidyl ester
CTLA-4	cytotoxic T-lymphocyte-associated protein 4
Cy	cyclophosphamide
ddPCR	droplet digital PCR
EF1 α	ubiquitous elongation factor 1 alpha
EFS	short version of ubiquitous elongation factor 1 alpha
GvHD	graft-versus-host disease
hFOXP3	human forkhead box P3
HLA	human leukocyte antigen
HSCT	hematopoietic stem cell transplantation
HSPC	hematopoietic stem/progenitor cell
i.p.	intraperitoneal
IPEX	immunodysregulation polyendocrinopathy enteropathy X-linked
IL	interleukin
LNGFR	long nerve growth factor receptor
MFI	mean fluorescence intensity
MOI	multiplicity of infection
NovB2	nodamuravirus B2 protein expression plasmid
PE	phycoerythrin
PBS	phosphate-buffered saline
PGK	phosphoglycerate promoter
qPCR	quantitative real time polymerase chain reaction
RPMI	Roswell Park Memorial Institute
Sf	<i>scurfy</i>
Tconv	conventional T cell
Tem	temsirolimus
Treg	regulatory T cell
VCN	vector copy number
WT	wild type

Introduction

Immunodysregulation polyendocrinopathy enteropathy X-linked (IPEX) syndrome is a primary immunodeficiency caused by mutations in the gene coding for the transcription factor forkhead box P3 (FOXP3) ^{1,2}. These mutations lead to the loss of function of CD4⁺CD25⁺ regulatory T cells (Treg), a small subset of CD4⁺ T cells dedicated to the control of immune response ³⁻⁵. Patients with IPEX develop of multiple autoimmune manifestations early in life ⁶. The current treatments for IPEX syndrome include supportive therapy, immunosuppressive therapy, and hematopoietic stem cell transplantation (HSCT). Immunosuppression is usually partially effective and is often limited by infectious complications and toxicities. At present, the only curative treatment is allogeneic HSCT. However, the lack of HLA-compatible donors and the patients' condition result in a high mortality. Effective alternative treatments are therefore urgently needed. From HSCT, we learned that partial donor chimerism and selective expansion of Treg are sufficient for complete remission ⁷⁻⁹.

Scurfy mice present a spontaneous *FoxP3* mutation. Within the first 10 days of life, these mice develop a fatal disease with organ specific auto-immunity ¹⁰ that reproduces the most severe IPEX syndrome. Various studies in *scurfy* mouse have demonstrated that the adoptive transfer of Treg within the first two days of life is an effective treatment ^{3,11}. However, no one has demonstrated that Treg transfer can cure *scurfy* disease. A new therapeutic strategy is required to broaden the therapeutic window and mimic the patient treatments.

Several gene therapies targeting mature T cells have been successfully developed ^{12,13}. In Rag-deficient mice, the retroviral or lentiviral transfer of *Foxp3* was sufficient to convert CD4⁺ T cells into suppressive lymphocytes able to control an inflammatory bowel disease ³. Furthermore, Passerini and al.'s demonstrated that the adoptive transfer of FOXP3-transduced CD4⁺ T cells prevented graft-versus-host disease (GvHD) in a Xenograft model ¹⁴. These preclinical studies suggest that the transfer of wild-type (WT) FOXP3 gene into T cells is a promising treatment (3,14). At present, two caveats prevent the translation of these preclinical studies into the clinic: the adoptive transfer of FoxP-3 transduced CD4⁺ T cells was used before the onset of autoimmune manifestations, and the FOXP3-transduced cells only partly reproduced the Treg's transcriptional signature and suppressive function ¹⁵. The expression of FOXP3 must be stable and strong enough to provide suppressive function and a surface marker is required to avoid adverse reactions related to the injection of non-corrected Tconv.

Here, we describe development and implementation of a full preclinical strategy for transferring FOXP3 into *scurfy* CD4⁺ T cells. We demonstrated that the resulting Treg were able to rescue disease manifestations in the *scurfy* model after the onset of autoimmune disease. This gene therapy strategy paves the way to clinical trials with curative intent in patients with IPEX.

Material and methods

Ethics

Animal procedures were approved by the animal committee (Paris University, 03/07/2017) and the Ministry of Agriculture (APAFIS#8440-2016062309559589). The procedures were performed in accordance with the EU Directive 2010/63/EU.

Mice

The *scurfy* phenotype was obtained by backcrossing on a B6.129S7-*Rag1*^{tm1Mom}/J background, allowing the generation of X^{Sf}/X^{Sf}.*Rag1*^{-/-} females. Crossing of these females with WT C57BL/6J mice resulted in only diseased X^{Sf}/Y.*Rag1*^{-/+} males. These males developed a *scurfy* phenotype. We developed a specific *scurfy* disease score ranging from 0 (no disease) to 21 (most severe disease) (see Supplemental Table 1).

Wild-type Treg

Splenocytes and lymph nodes were harvested from B6LY5.1 CD45.1 mice.

Scurfy CD4⁺ T cells

Lymph nodes were collected from 10-day-old *scurfy* mice, and CD4⁺ T cells were separated using a murine CD4⁺ T cell Isolation Kit (Miltenyi Biotec, Paris, France).

Lentiviral vectors

The cDNAs for a truncated codon-optimized human Δ LNGFR as a membranous reporter and a codon-optimized human FOXP3 were cloned into a pCCL backbone. We generated eight vectors in total: four expressing FOXP3 and the four corresponding mocks.

Two vectors had a bidirectional promoter architecture. One allowed FOXP3 expression under the control of EF1 α and Δ LNGFR expression under the control of PGK promoter (LNGFRp-eFOXP3 and LNGFRp-e, respectively), and the other allowed FOXP3 expression under the control of PKG and Δ LNGFR under the control of EFS (LNGFRp-pFOXP3 and LNGFRp-p, respectively). Two bicistronic vectors were created (using the 2A self-cleaving peptide system) to allow the co-expression of FOXP3 and Δ LNGFR (namely eLNGFR.t2a.FOXP3 and eLNGFR.t2a versus. eFOXP3.t2a.LNGFR and e.t2a.LNGFR) (Fig. 1A).

T cell transduction

T cell transduction was performed as previously describe¹⁶. Transduced cells were stained on day 5 post-transduction, using Δ LNGFR PE antibodies (clone ME20.4-1.H4, Miltenyi Biotec), and sorted on an SH800 system (Sony Biotechnology).

Adoptive T cell transfer

First, *scurfy* mice were treated with 2 mg/kg temsirolimus (LC Laboratories, Woburn, USA) via subcutaneous injections twice a week. An anti-CD3 Fab'2 (clone 145-2C11, BioXCell, West Lebanon, USA) was injected subcutaneous (20 µg/day) once a day for 5 days, starting on day 8 after birth. Cyclophosphamide (European Pharmacopoeia Reference Standard, Merck KGaA, Darmstadt, Germany) was injected i.p. at 50, 100, or 150 mg/kg 10 days after birth. On day 10 or day 14, CD4⁺CD25⁺ CD45.1⁺ cells or engineered CD4⁺ T cells from *scurfy* mice were injected i.p.. In the indicated experiments, human IL-2 (PROLEUKIN®, Novartis, Basel, Switzerland) was injected i.p. at 1000 IU/g once a day for 5 days and then once a week. A reference survival curve of untreated *scurfy* mice was generated from all experiments.

Transcriptomic analysis

On day 50, 1000 CD45.1 or LNGFR⁺ CD4⁺ T cells were sorted twice from lymph nodes (using a flow cytometer (SH800, Sony Biotechnology, Weybridge, UK)) directly into 5 µl lysis buffer. Smart-seq2 libraries for ultra-low-input RNA-seq were prepared as described previously^{17,18}. Samples were sequenced on an Illumina NextSeq500 system, using the 2 x 25 bp read option. Transcripts were quantified using the Broad Technology Labs computational pipeline (42). Normalized reads were further filtered and analyzed using Multiplot Studio in the GenePattern software (<https://www.genepattern.org/modules/docs/Multiplot/2>) and R Studio® (version 1.2.5019, RStudio Team 2020, PBC, Boston, MA, United States, <http://www.rstudio.com/>). To reduce noise, only genes with a coefficient of variation between biological replicates <0.3 in either comparison group, and with at least one sample with an expression value >30 were selected.

Statistical analysis

Data were described as the mean ± SD. All statistical analyses were performed with GraphPad Prism (version 8.0, GraphPad Software, Inc., San Diego, CA). Statistical tests included the non-parametric Mann-Whitney test, Fisher's exact test, and two-way ANOVA. The threshold for statistical significance was set to p<0.05.

Results

Conversion of *scurfy* CD4⁺ T cells into Treg by *FOXP3* gene transfer

Four distinct vectors were generated: two bidirectional vectors using either a phosphoglycerate (PGK)/ubiquitous elongation factor 1 alpha (EF1 α) (p-e) or a short version of EF1 α (EFS)/PGK (e-p) promoter cassette driving the expression of Δ LNGFR in the reverse orientation and FOXP3 in the forward position, and two bicistronic vectors using the T2A self-cleaving peptide system to co-express LNGFR and FOXP3, either LNGFR.t2a.FOXP3 or FOXP3.t2a.LNGFR (both driven by the EF1 α promoter) (Fig. 1A). The corresponding four mock vectors (driving the expression of Δ LNGFR only) were also generated.

The titers of the bidirectional vectors were more than 10 times higher than those of the bicistronic vectors (Fig. 1B). Five days after transduction at a multiplicity of infection of 10 (Fig. 1C), 5.2 to 25.2% of the WT CD4⁺ T cells expressed Δ LNGFR⁺. Spearman's coefficient (r^2) for the correlation between FOXP3 and Δ LNGFR expression was 0.51, 0.54, 0.66 and 0.61 for the LNGFRp-eFOXP3, LNGFR-eFOXP3, eLNGFR.t2a.FOXP3 and eFOXP3.t2a.LNGFR vectors, respectively. The eFOXP3.t2a.LNGFR vector was excluded from further evaluation because of its low transduction efficiency. The LNGFR-eFOXP3 construct gave a lower mean fluorescence intensity (MFI) for FOXP3 expression and was excluded. Both the LNGFRp-eFOXP3 and eLNGFR.t2a.FOXP3 constructs were tested in *scurfy* CD4⁺ T cells. As shown in Fig. 1D, the level of transduction after 5 days was significantly higher with the bidirectional LNGFRp-eFOXP3 construct than with the bicistronic eLNGFR.t2a.FOXP3 construct for both WT CD4⁺ T lymphocytes and *scurfy* CD4⁺ T lymphocytes ($p = 0.002$ and 0.007 , respectively). Importantly, the MFI of FOXP3 expression was similar for CD4^{LNGFRp-eFOXP3} and CD4^{eLNGFR.t2a.FOXP3} in WT cells but was significantly higher with the bidirectional LNGFRp-eFOXP3 construct, compared with the T2A construct in *scurfy* CD4⁺ T lymphocytes ($p=0.04$) (Fig. 1E). After sorting of transduced cell and expansion, the vector copy number (VCN) in WT CD4⁺ T lymphocytes ranged from 0.9 to 1.9 for the bidirectional vector and from 0.9 to 1.4 in *scurfy* CD4 T cells. *Scurfy* CD4⁺ T cells transduced with the T2A vector were significantly less viable, not allowing VCN quantification. Since the three criteria were met for LNGFRp-eFOXP3 and its mock counterpart LNGFRp-e, they two were selected for functional evaluation (referred to hereafter as LNGFR.FOXP3 and LNGFR).

A combination of cyclophosphamide, interleukin-2 and Treg cures *scurfy* syndrome

Hence, we sought to develop a new therapeutic approach to skew the immune response towards the regulatory arm by depleting activated Tconv and promoting Treg expansion.

To this end, we evaluated various immunosuppressive regimens, including temsirolimus (a prodrug for sirolimus that doubles life expectancy in *scurfy* mice¹⁹, anti-CD3 antibody, and cyclophosphamide (Cy). The experimental scheme consisted in injection of the immunosuppressive drug and then the transplantation of 5×10^5 congenic WT CD45.1 CD4⁺CD25^{high} Treg (Fig. S1A, D and G). To

reproducibly evaluate the *scurfy* mouse phenotype, we developed a specific *scurfy* disease score (Supplemental Table 1). Engraftment of WT Treg was quantified in various tissues at the study endpoint. When combined with Treg, temsirolimus and anti-CD3 did not significantly curb the course of *scurfy* disease (Fig. S1B and 1E). In contrast, a combination of Cy conditioning with Treg resulted in a significantly lower *scurfy* score, starting from 62 days of follow-up (Fig. S1H). Chimerism at endpoint seemed lower after Cy conditioning compared to chimerism after Te or anti-CD3 treatment (Fig. S1C, F and I). But it was evaluated at a later end-point (D77) thanks to a survival improvement with Cy treatment, while analyzed at D28 and D35 respectively for Te and anti-CD3 treatment. We thus selected Cy as immunosuppressive regimen, based on *scurfy* scores and survival.

The percentage of WT Treg remained low (less than 2% of CD4+ cells) in all the tissues analyzed, irrespective of the type of immunosuppressive drug used (Fig. S12C, F and I). We therefore sought to increase the engraftment of Treg by evaluate different dose levels of Cy (50, 100 or 150 mg/kg body weight (data not shown) administered intraperitoneally (i.p.) to *scurfy* males on day 10 of life. T cell depletion was similar for all three doses, with a nadir between 3 and 5 days after Cy injection. However, we observed growth retardation and transient alopecia, which were correlated with the dose of Cy. We therefore selected the lowest Cy dose (i.e. 50 mg/kg) in order to reduce drug toxicity. Treg transfer was performed on day 14 in mice conditioned with a single Cy injection on day 10 (Fig. S12G).

We next sought to further tip the balance in favor of Treg by promoting their expansion. On the basis of previous reports of a beneficial effect of low-dose interleukin (IL)-2 on Treg expansion²⁰⁻²², we treated *scurfy* recipients with IL-2 once a day for 5 days and then once a week (Fig. 2A). With the combination of Cy conditioning, Treg, and IL-2 injection, the *scurfy* score started to fall on day 22 after Treg transfer. The score on day 36 was significantly lower in treated mice (1.0 ± 0.3) than in control mice (4.2 ± 0.2) ($p=0.0001$ in an analysis of variance (ANOVA)) (Fig. 2B). Fifty days after Treg transfer, the CD45.1+ chimerism among CD4+ T cells was $2.2\% \pm 0.6$ in lymph nodes, $3.7\% \pm 1.4$ in the spleen, $2.1\% \pm 0.5$ in the blood, $3.5\% \pm 3.2$ in the liver, and $3.3\% \pm 0.8$ in the lung (Fig. 2C). Lastly, the survival time of Treg transferred mice (69 days) was greater than in Cy-treated mice (39 days; $p=0.0004$) and furthermore than non-treated mice (PBS, 28 days; $p<0.0001$) (Fig. 2D). Interestingly, treatment with Cy+IL-2 alone was associated with longer survival (median survival time: 51 days), despite the lack of FOXP3+ CD4+ T cells ($p=0.03$). As additional evidence of Treg-induced homeostatic control of the host immune system, resident T CD4+ T cells maintained a CD62L+ naïve compartment in Treg-treated mice but not in control mice (Fig. 2E).

This is the first evidence to show that delayed Treg administration in combination with Cy-conditioning and low dose IL-2 can improve outcomes in *scurfy* mice.

***Scurfy* CD4+ T cells transduced with the LNGFR.FOXP3 vector rescue *scurfy* mice**

We next used our adoptive transfer model to evaluate the ability of transduced CD4^{LNGFR.FOXP3} cells to control *scurfy* disease. Firstly, in order to assess the dose of CD4^{LNGFR.FOXP3} cells required, Cy-conditioned *scurfy* males were injected at the age of 14 days with congenic 5x10⁵ CD45.1 Treg or 5x10⁵, 7.5x10⁵ or 1x10⁶ *scurfy* CD4^{LNGFR.FOXP3} cells. The results were not significant between the three different doses and WT Treg. Importantly, one mouse was sacrificed before reaching the 49 days endpoint in the 1x10⁶ dose group because of severe *scurfy* injury. Therefore, the mean score at endpoint was under-evaluated in this arm. In addition, the chimerism was higher in the 7.5x10⁵ group with 4.0% in the blood compared to the 1x10⁶ group and 5x10⁵ group (with respectively 1.2% and 0.6%, Fig. S2B and C). For those reasons, the dose of 7.5x10⁵ CD4^{LNGFR.FOXP3} was selected for further evaluation. The naïve CD4⁺ T cell compartment (characterized by CD62L staining) was restored to a similar extent by the three doses of CD4^{LNGFR.FOXP3} (Fig. S2D).

Adoptive transfer experiments with 5x10⁵ WT Treg, 7.5x10⁵ CD4^{LNGFR.FOXP3} cells, 7.5x10⁵ CD4^{LNGFR} cells and vehicle (phosphate-buffered saline (PBS)) was assessed. All mice received Cy and IL-2. The VCN of CD4^{LNGFR.FOXP3} and CD4^{LNGFR} ranged from 1.2 to 1.5. Mice were carefully monitored until sacrifice on day 50. *Scurfy* score rose above 7 in all groups in a similar manner, up to day 27 (Fig. 3A). By day 32, the mean \pm standard deviation (SD) score had risen towards the endpoint to the same extent in mice that received Cy and IL-2 alone or CD4^{LNGFR} cells but was significantly lower in mice treated with WT Treg and CD4^{LNGFR.FOXP3} cells (6.5 \pm 0.5 and 4.5 \pm 0.5, respectively; p=0.007 and 0.0008; respectively). More specifically, mice having received WT Treg and CD4^{LNGFR.FOXP3} cells gained weight, improved eczema on the tail and blepharitis, and recovered from Cy-induced alopecia. In contrast, mice having received vehicle or CD4^{LNGFR} cells failed to thrive and presented severe eczema over the whole body (Fig. S3A).

On day 50, chimerism analysis showed that the mean percentage of CD45.1 WT Treg was 5% (1.7 - 12.6%) in lymph nodes, spleen, blood, liver, and lung (Fig. 3B). In mice treated with CD4^{LNGFR.FOXP3} T cells, the percentage of chimerism was slightly lower, with a mean value of 3.4% (0.2 - 4.6%) in lymph nodes, spleen, blood, liver, and lung (Fig. 3C). In contrast, CD4^{LNGFR} T cells did not expand, and percentage of chimerism remained below 1.5% in all tissues. Importantly, human FOXP3 expression in the lymph nodes was maintained 50 days after adoptive transfer in animals treated with Δ LNGFR⁺ CD4⁺ cells (Fig. S3B). The Δ LNGFR⁺ cells were sorted from the lymph nodes, and the mean \pm SD VCN was 2.3 \pm 0.8 in CD4^{LNGFR.FOXP3} T cells and 1.6 \pm 0.7 in CD4^{LNGFR} T cells (Fig. S3C).

CD62L staining of the lymph nodes (Fig. S3D) demonstrated that a subset of naïve CD4⁺ T cells had been restored and maintained in mice treated with Treg and CD4^{LNGFR.FOXP3} cells. The percentage of CD62L⁺ cells was 15.7 \pm 0.6% in CD4⁺ T cells from *scurfy* mice treated with Cy and IL-2 and 78.1 \pm 2.4% in WT mice. Adoptive transfer of Treg or CD4^{LNGFR.FOXP3} T cells in *scurfy* mice increased the percentage CD62L⁺ cells to 44.0 \pm 6.2% and 31.1 \pm 11.8%, respectively, while adoptive transfer of CD4^{LNGFR} T cells maintained the level at 20.8 \pm 2.5% (Fig. S3D).

Survival was significantly extended following CD4^{LNGFR.FOXP3} treatment, relative to Cy-treated *scurfy* mice; the median survival times were 83 and 47 days, respectively (p=0.0195). Median survival was significantly longer with WT Treg (90 days)—than with Cy alone (47 days) (p<0.0001). Median survival for Treg treated mice did not differ significantly from that in CD4^{LNGFR.FOXP3}-treated mice (p=0.285). Likewise, PBS- and CD4^{LNGFR}-treated mice did not differ significantly in their survival, with median survival times of 54.5 and 53 days, respectively (p=0.8729) (Fig. 3D). After 110 days of follow-up, the degree of chimerism in CD4⁺ T cells from the CD45.1 Treg and CD4^{LNGFR.FOXP3} groups was lower than on day 50, with mean values of 1.5% and 1.1%, respectively (Fig. S3E). Importantly, human forkhead box P3 (hFOXP3) could still be detected in CD4^{LNGFR.FOXP3} T cells - demonstrating the *in vivo* stability of this protein in transduced *scurfy* CD4⁺ T cells.

Overall, these results demonstrated that FOXP3 expression in *scurfy* CD4⁺ T cells recapitulated suppressor function and transduced CD4^{LNGFR.FOXP3} cells were able to rescue mice from *scurfy* autoimmune disease.

LNGFR.FOXP3-expressing *scurfy* CD4⁺ T cells significantly recapitulate Treg transcriptomic profile

To determine whether the engineered CD4^{LNGFR.FOXP3} cells mimicked *bona fide* Treg, we explored their transcriptomic profile 35 days after adoptive transfer in *scurfy* recipients. FOXP3-transduced CD4⁺ T cells have been analyzed before but only after *in vitro* culture; our present experiments were designed to reveal the effect of transducing with cells that have settled *in vivo*, i.e. the direct impact of FOXP3 and secondary cell adaptations *in vivo*. We thus purified RNA from rescued *scurfy* mice CD4^{LNGFR.FOXP3}, CD4^{LNGFR} T cells and WT Treg for low-input RNAseq transcriptomic analyses. Several important observations were made. Firstly, the RNAseq reads distinguished between the transduced human *FOXP3* and the endogenous murine *Foxp3* (Fig. S4A). Human *FOXP3* transcripts were detected in all CD4^{LNGFR.FOXP3} samples at levels (~1,000 arbitrary units) that were somewhat higher than in normal human blood Treg (typically ~150-200 in our studies; Fig. S4A). Mouse *Foxp3* transcripts were also detected at slightly higher levels in CD4^{LNGFR.FOXP3} cells than in CD4^{LNGFR} cells, although these levels were still much lower than in normal murine Treg (Fig. S4B). Secondly, a comparison of the gene expression profiles of CD4^{LNGFR.FOXP3} and CD4^{LNGFR} cells showed that FOXP3 induced a significant shift towards the prototypic transcriptional signature of Treg²³ (Fig. 4A; p=0.005 and p=0.003 for the upregulated and downregulated signatures, respectively). The direct comparison of Treg signature genes in CD4^{LNGFR.FOXP3} and Treg cells (Fig. S4C) confirmed that upregulated transcripts were generally less expressed in CD4^{LNGFR.FOXP3} cells than in WT Treg (this was most clear for *Foxp3* and *Gpr83*), and that downregulated transcripts were less expressed in WT Treg than in CD4^{LNGFR.FOXP3} cells.

A focus on core Treg transcripts (unpublished data; Figure 4B) showed that their levels varied significantly in CD4^{LNGFR.FOXP3} cells: some were expressed at levels similar to those seen in WT Treg

(e.g. *Tnfrsf9*, *Capg*, and *Ctla4*), whereas others were underexpressed (e.g. *Gpr83*, *Ikzf2*, *Tnfrsf1b*, and *Foxp3*). To provide a quantitative estimate, we computed a core Treg “signature score” (Fig. 4C and Table S2), where 0 and 1 correspond to expression in Tconv and Treg cells, respectively). This score varied strongly, with some transcripts being induced to full Treg levels (*Ctla4*, *Capg*) and others less so (*Gpr83*, *Ikzf2*), giving a median [interquartile range] score of 0.41 [0.25-0.74].

More generally, we also examined the transcripts differentially expressed in CD4^{LNGFR.FOXP3} cells versus CD4^{LNGFR} cells (those with a fold-change (FC)>2 and a nominal p<0.01). The heat map (Fig. 4D) highlighted the induction of Treg signature genes in CD4^{LNGFR.FOXP3} cells and also the presence of a large gene cluster of overexpressed transcripts (relative to Treg cells). A pathway analysis showed that these overexpressed transcripts were involved in cell cycling (Fig. 4D). We hypothesize that this CD4^{LNGFR.FOXP3} population must be actively cycling - perhaps in response to homeostatic control that strongly drives Treg expansion in deficient environments. Thus, an analysis of the transcriptome revealed the lasting but partial restoration of Treg identity in FOXP3-transduced *scurfy* cells – even in the persistently inflammatory environment.

Discussion

Here, we described our development of a new Treg adoptive transfer model in the *scurfy* mouse. This model enables the long-term functional assessment of T-cell-based gene therapy approaches for Foxp3-deficient autoimmune disease. Using a bidirectional lentiviral vector, we showed that *FOXP3* gene transfer in *scurfy* CD4⁺ T cells generated potent, stable regulatory T cells that recapitulated most of the Treg’s transcriptomic profile and rescued the *scurfy* syndrome.

Previously, the transfer of splenocytes, Treg or induced Treg in *scurfy* mice has been shown to prevent the development of *scurfy* symptoms^{3,11,24}. However, there are no previous reports of rescue after symptoms have developed. Our results demonstrated that Treg transfer after the appearance of symptoms rescued *scurfy* symptoms. This was achieved by Cy conditioning prior to Treg injection and repeated IL-2 injections to favor Treg expansion. In this model, we observed Treg engraftment, a significantly lower clinical score, and, a three-fold longer survival time (around 100 days).

Of the various Treg adoptive transfer strategies tested here, Cy conditioning was associated with the best control of autoimmunity. Cyclophosphamide has been shown to deplete the T cell niche in mice^{25,26}. Moreover, Cy inhibits the function of activated T cells and thus results in a relative enrichment in Treg^{27,28}. However, even low dose levels of Cy resulted in adverse events in young mice. To tip the balance between Treg and Tconv in clinical applications, another type of conditioning would be required as anti-CD3 or anti-TCR antibodies. Those strategies would allow a selective depletion of activated T cells sparing other cells subsets and limiting side-effects. However, anti-CD3 antibody was not sufficient in our model to reach an adequate level of Tconv depletion. Furthermore, low dose IL-2 has been shown to favor Treg expansion in the context of type I diabetes²⁹, systemic lupus

erythematous³⁰ and several other autoimmune diseases^{31–33}. Interleukin-2 also enhances the proliferation of donor-specific Treg and promotes tolerance in allogeneic transplantation^{34,35}. The safety and biological efficacy of low-dose IL-2 as a Treg inducer in a set of 14 autoimmune diseases was assessed in the TRANSREG study³². Similarly, to this study, the initial induction in our mouse model was followed by weekly maintenance injections of IL-2. Importantly, treatment with low-dose IL-2 did not worsen auto-immunity in *scurfy* mice - suggesting that it is possible to maintain IL-2 treatment in patients. Moreover, we observed a trend toward an extended survival with IL-2 alone. We hypothesized treatment with IL-2 could expand a cell subset with suppressive properties even in the absence of FOXP3 expression (work in progress).

In our model of Treg adoptive transfer, the CD4⁺ T cells transduced with the LNGFR.FOXP3 vector were able to rescue the *scurfy* disease - demonstrating the lentiviral vector's efficiency to restore regulatory function. Interestingly, *scurfy* CD4⁺ T cells transduced with LNGFR.FOXP3 vector expanded more readily than those transduced with the mock LNGFR vector. This increased sensitivity to IL-2 might have been due to a higher level of CD25 expression demonstrated by flow cytometry (not shown) and in transcriptomic data (Figure 4A-C). Moreover, these adoptively transferred Treg were stably maintained for 110 days in an inflammatory context, expressed FOXP3 in a lasting manner, and thus kept their regulatory profile. Importantly, a transcriptomic analysis demonstrated that hFOXP3 expression was associated with the induction of mFOXP3 - suggesting that the homology between human and murine FOXP3 allows the human protein to act as a transcription factor in murine CD4⁺ T cells.

In our assay, *scurfy* disease was controlled slightly better by the transfer of WT Treg than by the transfer of CD4^{LNGFR.FOXP3} cells. The difference might be explained by firstly, the level of chimerism with CD4^{LNGFR.FOXP3} cells was half that seen with WT Treg. Secondly, our vector expressed human *FOXP3* at a lower level than murine *Foxp3* in WT Treg (despite higher level compared to human WT Treg, Fig. S4); this may explain why the CD4^{LNGFR.FOXP3} cells do not fully recapitulate the murine Treg's transcriptomic program. However, the proportion of cells expressing human FOXP3 in the present study was higher than previously reported²³. Thirdly, the engineered regulatory CD4⁺ T cells were collected from *scurfy* mice, activated *in vitro* for 5 days. This issue would require an optimization of manufacturing procedure to reduce cell activation and improve Treg retargeting of CD4⁺ T cells. Preselecting naïve T cells might result in more effective suppressor activity¹⁴. In the present study, some of the *scurfy* mice died (mostly from the recurrence of *scurfy* symptoms). Therefore, improvement of cell manufacturing to preserve naïve or T stem cell would be interesting to improve long-term latency of transduced cells. Moreover, multiple injections of Treg, higher dose levels of IL-2 and/or more frequent injections of IL-2 or IL-2 mutein to preferentially expand suppressive cells could be interesting to improve *scurfy* disease control.

Our present results demonstrated the feasibility of a T-cell based gene therapy approach for restoring CD4⁺ T cells' suppressive properties and controlling a severe autoimmune condition. Recently, Masiuk and al. developed a hematopoietic stem/progenitor cell (HSPC)-based model of gene therapy using a lentiviral vector expressing FOXP3 under the control of its endogenous promoter ³⁶. *Scurfy* HSPCs were engineered using this FOXP3 lentiviral vector and transplanted into WT mice, to produce corrected CD4⁺ T cells. The CD4^{FOXP3} cells demonstrated their ability to prevent the onset of *scurfy* phenotype. The total number of corrected *scurfy* CD4⁺ T cells injected in *scurfy* neonates was over 1.8x10⁷ and a VCN ranging from 3.3 to 5.8. Our genetic engineering of CD4⁺ T cells obtained a curative effect with a slightly lower cell dose and a lower VCN. These results demonstrated the feasibility of a HSPC gene therapy but suggest that FOXP3 expression driven by the endogenous promoter might require a higher VCN and a higher CD4⁺ cell dose. Gene therapy with CD4⁺ T cells expressing FOXP3 under the control an ubiquitous promoter and gene therapy with HSPCs expressing FOXP3 under the control of its own promoter are strategies that could be used separately or serially, depending on the patient profile. Gene editing in HSPCs might also be an alternative approach for full recapitulation of the Treg ontogeny ³⁷. However, treatment with genetically engineered CD4⁺ T cells would require mild conditioning and would then be applicable to severely diseased IPEX patients as a full curative therapy but also as a potential bridge therapy toward stem cell gene therapy in the more severely disease patients ⁶.

Acknowledgement

We are grateful to Aurélie Dujardin, Camila Piat, Laura Zapata, Jennifer Alonso and Emilie Panafieu from the SFR Necker animal facility, Sophie Berissi, Noémie Gadessaud and Sonita Ing from the SFR Necker histology facility, and Olivier Pellé and Corinne Cordier from the SFR Necker cytometry facility. We also thank Gisèle Froment, Didier Nègre and Caroline Costa from the lentiviral production facility/SFR BioSciences Gerland-Lyon Sud (UMS3444/US8).

This work was funded by a European Research Council grant (Gene for Cure: E16145KK).

Authorship Contributions

Marianne Delville: Conceptualization, Methodology, Investigation, Formal analysis, Writing - Original Draft, Writing - Review & Editing

Florence Bellier: Investigation, Formal analysis

Juliette Leon: Conceptualization, Methodology, Investigation, Formal analysis, Writing - Original Draft, Writing - Review & Editing

Roman Klifa: Investigation, Formal analysis

Sabrina Lizot: Investigation, Formal analysis

Hélène Vinçon: Investigation, Formal analysis

Steicy Sobrino: Investigation

Romane Thouennon: Investigation

Armance Marchal: Investigation

Alexandrine Guarrigue: Investigation

Juliette Olivré: Investigation

Soëli Charbonnier: Investigation

Chantal Lagresle-Peyrou: Conceptualization, Methodology, Writing - Review & Editing

Mario Amendola: Conceptualization, Methodology

Axel Schambach: Conceptualization, Methodology

David Gross: Conceptualization, Methodology

Baptiste Lamarthée: Investigation, Formal analysis, Writing - Review & Editing

Christophe Benoist: Conceptualization, Methodology, Writing - Review & Editing, Supervision

Julien Zuber: Conceptualization, Methodology, Writing - Review & Editing, Supervision

Marina Cavazzana: Conceptualization, Methodology, Writing - Review & Editing, Supervision, Funding acquisition

Isabelle André: Conceptualization, Methodology, Writing - Review & Editing, Supervision

Emmanuelle Six: Conceptualization, Methodology, Writing - Review & Editing, Supervision

Disclosure of Conflicts of Interest

Authors disclose no conflict of interest

Data sharing

Data have been deposited in GEO under accession number GSE166017.

References

1. Wildin RS, Ramsdell F, Peake J, et al. X-linked neonatal diabetes mellitus, enteropathy and endocrinopathy syndrome is the human equivalent of mouse scurfy. *Nat. Genet.* 2001;27(1):18–20.
2. Bennett CL, Christie J, Ramsdell F, et al. The immune dysregulation, polyendocrinopathy, enteropathy, X-linked syndrome (IPEX) is caused by mutations of FOXP3. *Nat. Genet.* 2001;27(1):20–21.
3. Fontenot JD, Gavin MA, Rudensky AY, Hughes H. Foxp3 programs the development and function of CD4+CD25+ regulatory T cells. 2003;
4. Hori S, Nomura T, Sakaguchi S. Control of regulatory T cell development by the transcription factor Foxp3. *Science.* 2003;299(5609):1057–1061.
5. Khattri R, Cox T, Yasayko S-A, Ramsdell F. An essential role for Scurfin in CD4+CD25+ T regulatory cells. *Nat. Immunol.* 2003;4(4):337–342.
6. Barzaghi F, Amaya Hernandez LC, Neven B, et al. Long-term follow-up of IPEX syndrome patients after different therapeutic strategies: An international multicenter retrospective study. *J. Allergy Clin. Immunol.* 2018;141(3):1036-1049.e5.
7. Kasow KA, Morales-Tirado VM, Wichlan D, et al. Therapeutic in vivo selection of thymic-derived natural T regulatory cells following non-myeloablative hematopoietic stem cell transplant for IPEX. *Clin. Immunol.* 2011;141(2):169–176.
8. Seidel MG, Fritsch G, Lion T, et al. Selective engraftment of donor CD4+25high FOXP3-positive T cells in IPEX syndrome after nonmyeloablative hematopoietic stem cell transplantation. *Blood.* 2009;113(22):5689–5691.
9. Horino S, Sasahara Y, Sato M, et al. Selective expansion of donor-derived regulatory T cells after allogeneic bone marrow transplantation in a patient with IPEX syndrome. *Pediatr. Transplant.* 2014;18(1):E25-30.
10. Godfrey VL, Wilkinson JE, Russell LB. X-linked lymphoreticular disease in the scurfy (sf) mutant mouse. *Am. J. Pathol.* 1991;138(6):1379–87.
11. Haribhai D, Williams JB, Jia S, et al. A Requisite Role for Induced Regulatory T cells in Tolerance Based on Expanding Antigen Receptor Diversity Dipica. *Immunity.* 2012;35(1):109–122.
12. Kalos M, June CH. Adoptive T cell transfer for cancer immunotherapy in the era of synthetic biology. *Immunity.* 2013;39(1):49–60.
13. June CH, Sadelain M. Chimeric antigen receptor therapy. *N. Engl. J. Med.* 2018;379(1):64–73.
14. Passerini L, Mel ER, Sartirana C, et al. CD4+ T cells from IPEX patients convert into

- functional and stable regulatory T cells by FOXP3 gene transfer. *Sci. Transl. Med.* 2013;5(215):.
15. Fu W, Ergun A, Lu T, et al. A multiply redundant genetic switch “locks in” the transcriptional signature of regulatory T cells. *Nat. Immunol.* 2012;13(10):972–980.
 16. Delville M, Soheili T, Bellier F, et al. A Nontoxic Transduction Enhancer Enables Highly Efficient Lentiviral Transduction of Primary Murine T Cells and Hematopoietic Stem Cells. *Mol. Ther. - Methods Clin. Dev.* 2018;10:341–347.
 17. Picelli S, Björklund ÅK, Faridani OR, et al. Smart-seq2 for sensitive full-length transcriptome profiling in single cells. *Nat. Methods.* 2013;10(11):1096–1100.
 18. Picelli S, Faridani OR, Björklund ÅK, et al. Full-length RNA-seq from single cells using Smart-seq2. *Nat. Protoc.* 2014;9(1):171–181.
 19. Chen C, Liu YY, Liu YY, Zheng P. Mammalian target of rapamycin activation underlies HSC defects in autoimmune disease and inflammation in mice. *J. Clin. Invest.* 2010;120(11):4091–4101.
 20. Serreze D V, Hamaguchi K, Leiter EH. Immunostimulation circumvents diabetes in NOD/Lt mice. *J. Autoimmun.* 1989;2(6):759–76.
 21. Tang Q, Adams JY, Penaranda C, et al. Central role of defective interleukin-2 production in the triggering of islet autoimmune destruction. *Immunity.* 2008;28(5):687–97.
 22. Grinberg-Bleyer Y, Baeyens A, You S, et al. IL-2 reverses established type 1 diabetes in NOD mice by a local effect on pancreatic regulatory T cells. *J. Exp. Med.* 2010;207(9):1871–8.
 23. Hill JA, Feuerer M, Tash K, et al. Foxp3 Transcription-Factor-Dependent and -Independent Regulation of the Regulatory T Cell Transcriptional Signature. *Immunity.* 2007;27(5):786–800.
 24. Huter EN, Punksody GA, Glass DD, et al. TGF- β -induced Foxp3+ regulatory T cells rescue scurfy mice. *Eur. J. Immunol.* 2008;38(7):1814–1821.
 25. Huyan X-H, Lin Y-P, Gao T, Chen R-Y, Fan Y-M. Immunosuppressive effect of cyclophosphamide on white blood cells and lymphocyte subpopulations from peripheral blood of Balb/c mice. *Int. Immunopharmacol.* 2011;11(9):1293–1297.
 26. Salem ML, Al-Khami AA, El-Nagaar SA, et al. Kinetics of rebounding of lymphoid and myeloid cells in mouse peripheral blood, spleen and bone marrow after treatment with cyclophosphamide. *Cell. Immunol.* 2012;276(1–2):67–74.
 27. Zhang H, Chua KS, Guimond M, et al. Lymphopenia and interleukin-2 therapy alter homeostasis of CD4 + CD25 + regulatory T cells. *Nat. Med.* 2005;11(11):1238–1243.
 28. Wachsmuth LP, Patterson MT, Eckhaus MA, et al. Posttransplantation cyclophosphamide prevents graft-versus-host disease by inducing alloreactive T cell dysfunction and suppression. *J. Clin. Invest.* 2019;129(6):2357–2373.
 29. Hulme MA, Wasserfall CH, Atkinson MA, Brusko TM. Central Role for Interleukin-2 in Type 1 Diabetes. *Diabetes.* 2012;61(1):14–22.

30. von Spee-Mayer C, Siegert E, Abdirama D, et al. Low-dose interleukin-2 selectively corrects regulatory T cell defects in patients with systemic lupus erythematosus. *Ann. Rheum. Dis.* 2016;75(7):1407–15.
31. Saadoun D, Rosenzwajg M, Joly F, et al. Regulatory T-Cell Responses to Low-Dose Interleukin-2 in HCV-Induced Vasculitis. *N. Engl. J. Med.* 2011;365(22):2067–2077.
32. Rosenzwajg M, Lorenzon R, Cacoub P, et al. Immunological and clinical effects of low-dose interleukin-2 across 11 autoimmune diseases in a single, open clinical trial. *Ann. Rheum. Dis.* 2019;78(2):209–217.
33. Mahmoudpour SH, Jankowski M, Valerio L, et al. Safety of low-dose subcutaneous recombinant interleukin-2: systematic review and meta-analysis of randomized controlled trials. *Sci. Rep.* 2019;9(1):7145.
34. Koreth J, Matsuoka K, Kim HT, et al. Interleukin-2 and Regulatory T Cells in Graft-versus-Host Disease. *N. Engl. J. Med.* 2011;365(22):2055–2066.
35. Betts BC, Pidala J, Kim J, et al. IL-2 promotes early Treg reconstitution after allogeneic hematopoietic cell transplantation. *Haematologica.* 2017;102(5):948–957.
36. Masiuk KE, Laborada J, Roncarolo MG, Hollis RP, Kohn DB. Lentiviral Gene Therapy in HSCs Restores Lineage-Specific Foxp3 Expression and Suppresses Autoimmunity in a Mouse Model of IPEX Syndrome. *Cell Stem Cell.* 2019;24(2):309-317.e7.
37. Goodwin M, Lee E, Lakshmanan U, et al. CRISPR-based gene editing enables FOXP3 gene repair in IPEX patient cells. *Sci. Adv.* 2020;6(19):.
38. Zemmour D, Zilionis R, Kiner E, et al. Single-cell gene expression reveals a landscape of regulatory T cell phenotypes shaped by the TCR. *Nat. Immunol.* 2018;19(3):291–301.
39. Maetzig T, Galla M, Brugman MH, et al. Mechanisms controlling titer and expression of bidirectional lentiviral and gammaretroviral vectors. *Gene Ther.* 2010;17(3):400–411.

Figures' legends

Figure 1. The efficiency of FOXP3 expression by lentiviral vectors

A. Vector maps showing the design of the four vectors and their mock counterparts within the pCCL backbone:

- two bidirectional vectors:
 - LNGFRp-eFOXP3 expressing FOXP3 under the control of EF1 α promoter and expressing the reporter protein Δ LNGFR under the control of PGK promoter, and its mock counterpart LNGFRp-e.
 - LNGFR-eFOXP3 expressing FOXP3 under the control of PGK promoter and expressing the reporter protein Δ LNGFR under the control of the EFS promoter, and its mock counterpart LNGFR-e-p.
- two bicistronic vectors under the control of EF1 promoter, both based on a self-cleaving T2A sequence:
 - eLNGFR.t2a.FOXP3 and its mock counterpart eLNGFR.t2a.
 - eFOXP3.t2a.LNGFR, and its mock counterpart e.t2a.LNGFR.

LTR: long terminal repeat; WPRE6*: woodchuck hepatitis virus post-transcriptional regulatory element; PolyA unid: unidirectional poly-adenylation sequence; SIN: self-inactivating.

B. Quantification of the titers of vector used for transduction.

C. Representative flow cytometry dot plots showing the expression of human FOXP3 and Δ LNGFR on WT murine CD4⁺ T cells 5 days after transduction with all the constructs expressing FOXP3. The correlation between FOXP3 expression and Δ LNGFR expression was quantified by calculating Spearman's correlation coefficient ($r^2=0.51, 0.54, 0.66$ and 0.61 for the LNGFRp-eFOXP3, LNGFR-eFOXP3, eLNGFR.t2a.FOXP3, and eFOXP3.t2a.LNGFR vectors, respectively).

D. Transduction efficacy quantified as the percentage of Δ LNGFR on day 5 after transduction in WT and *scurfy* CD4⁺ T cells. Transduction efficiency was significantly higher with the LNGFRp-eFOXP3 vector than with the LNGFR.t2a.FOXP3 vector for both WT CD4⁺ T cells (black circles) and *scurfy* CD4⁺ T cells (grey squares) ($p=0.002$ and 0.007 , respectively, in a Mann-Whitney test:). In contrast, transduction efficacy with the mock vectors was higher with the T2A construct ($p=0.02$ and 0.04 in WT and *scurfy* CD4⁺ T cells, respectively). $n=3$ independent experiments for WT CD4⁺ T cells and $n=2$ independent experiments for *scurfy* CD4⁺ T cells.

E. The geometric MFI for FOXP3 expression was quantified on day 5 post-transduction (gated on CD4⁺ Δ LNGFR⁺) in WT cells (black circles) or *scurfy* cells (grey squares). The hFOXP3 MFI in WT CD4⁺ T cells was similar with LNGFRp-eFOXP3 and LNGFR.t2a.FOXP3 vectors. The MFI was significantly higher in *scurfy* CD4⁺ T cells transduced with LNGFRp-eFOXP3 vector than in the same

cell type transduced with LNGFR.t2a.FOXP3 ($p=0.04$ in a Mann-Whitney test). $n=3$ independent experiments for WT CD4⁺ T cells and $n=2$ independent experiments for *scurfy* CD4⁺ cells.

Figure 2. A specific combination of cyclophosphamide conditioning, IL-2 treatment and Treg transfer rescues *scurfy* syndrome

A. Rescue of *scurfy* mice

Scurfy males ($X^{Sf}/Y.Rag1^{+/-}$ on a CD45.2 background) were conditioned by an i.p. injection of 50 mg/kg cyclophosphamide on day 10 and then received 5×10^5 congenic CD45.1 WT Treg on day 14. Next, 1000 IU/g IL-2 was injected i.p. once a day for 5 days and then once a week. In an initial experiment, all mice were sacrificed on day 50 for flow cytometry analysis. Survival was analyzed in a second experiment ($n=3$ mice per group).

B. The *scurfy* disease score was rated (as described in the Methods) in Treg-treated mice (grey squares) and vehicle (PBS)-treated mice (black triangles). Differences were apparent after day 31 ($p=0.003$ in a Mann-Whitney test) and after day 38 ($p<0.001$). Cy: cyclophosphamide; IL: interleukin.

C. Flow cytometry analysis of CD45.1 chimerism, gated on CD4⁺ T cells in the lymph nodes, spleen, blood, liver, and lung. Cy: cyclophosphamide; IL: interleukin ($n=3$ mice per group).

D. Survival of *scurfy* mice untreated (PBS, plain dark line), treated with Cy only (Cy, continuous grey line), Cy and IL-2 (Cy+IL-2+PBS; dashed grey line) or Cy, IL-2 and 5×10^5 Treg (Cy+IL-2+Treg; pink line). There was a significant difference ($p=0.0004$ in a log rank test) between Cy+IL-2+PBS and Cy+IL-2+Treg groups ($n=6$ mice per group).

E. A representative flow cytometry histogram of CD62L expression, gated on CD4⁺ T cells in mice that had received Treg (dark grey) or vehicle (light grey). Cy cyclophosphamide; IL: interleukin ($n=3$ mice per group).

Figure 3. *Scurfy* CD4 T cells engineered with an LNGFR.FOXP3 vector rescue *scurfy* mice after disease onset

Male *scurfy* mice ($X^{Sf}/Y.Rag1^{+/-}$ on a CD45.2 background) were conditioned by an i.p. injection of 50 mg/kg of Cy on day 10 and then received either vehicle (grey circle), 5×10^5 congenic CD45.1 WT Treg (salmon square), CD4^{LNGFR} transduced *scurfy* cells (purple triangle) or 0.75×10^6 CD4^{LNGFR.FOXP3} transduced *scurfy* cells (blue triangle) on day 14. Next, 1000 IU/g IL-2 were injected i.p. once a day for 5 days and then once a week. Data from at least two independent experiments are shown.

A. The mean \pm SD *scurfy* disease score in mice treated with Treg, CD4^{LNGFR}, and CD4^{LNGFR.FOXP3}, versus vehicle-treated mice (p=0.01, 0.26 and 0.02 in a Mann-Whitney test, respectively) on day 42 (n \geq 3 per group).

B. All the mice were sacrificed on day 50 for flow cytometry analysis. CD45.1 chimerism was analyzed on day 50 (gated on CD4⁺ T cells) for the lymph nodes, spleen, blood, liver, and lung in mice receiving WT Treg or PBS.

C. Δ LNGFR chimerism was analyzed on day 50 (gated on CD4⁺ T cells) in the lymph nodes, spleen, blood, liver, and lung in mice receiving CD4^{LNGFR.FOXP3} cells, CD4^{LNGFR} cells or PBS. The level of chimerism was higher in CD4^{LNGFR.FOXP3}-treated mice than in CD4^{LNGFR}-treated mice (p=0.001).

D. Survival of *scurfy* mice from two independent experiments. Treatment with IL-2 did not increase survival relative to treatment with Cy or CD4^{LNGFR} cells. Mice treated with Treg and CD4^{LNGFR.FOXP3} cells survived for significantly lower than Cy-treated mice (p<0.0001 and 0.0195, respectively; n \geq 5 per group). Follow-up was continued up to 110 days.

Figure 4. CD4^{LNGFR.FOXP3} cells partly maintain the Treg signature after adoptive transfer on day 50 of life.

All the transcriptomic data came from a single experiment in which CD4^{LNGFR.FOXP3} cells, CD4^{LNGFR} cells and WT Treg were isolated from the corresponding treated mice (respectively n=4, n=2, and n=2) euthanized at 50 days old.

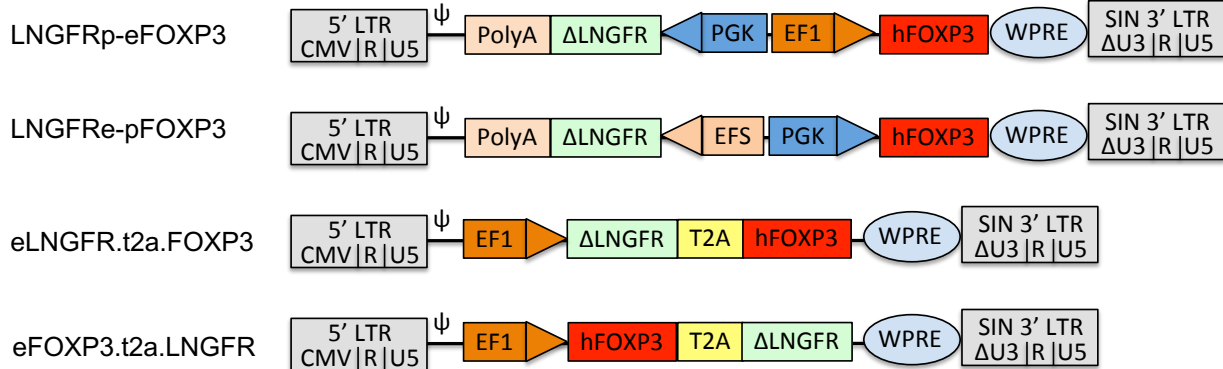
A. A volcano plot (the FC versus the *p* value) of the transcriptomes of CD4^{LNGFR.FOXP3} vs. CD4^{LNGFR} cells on day 50. The Treg upregulated signature (in red), downregulated signature (in blue)²³ and core Treg gene annotations are highlighted³⁸. The values in the upper half represent the number of corresponding Treg signature genes induced (right) or repressed (left), with the number of upregulated signature genes in red and the number of downregulated signature genes in blue. P-values for the Treg signature enrichment were obtained in a chi-squared test.

B. A heat map showing expression of the core Treg genes³⁸. The values correspond to the FC for each gene in each sample, normalized against the mean value for CD4^{LNGFR} cells.

C. The Treg signature score for the core Treg genes³⁸ in CD4^{LNGFR.FOXP3} cells, where 0 and 1 correspond to expression in Tconv (CD4.LNGFR) cells and Treg cells, respectively. The mean \pm SD signature score for CD4^{LNGFR.FOXP3} cells is represented.

D. A heat map showing all the significant differentially expressed genes (absolute FC >2, p<0.05) when comparing CD4^{LNGFR.FOXP3} cells with CD4^{LNGFR} cells (n=677). The -log₁₀ FC for the three groups of mice is shown. The Treg downregulated signature belongs to the most downregulated genes (green). Most of the upregulated genes are involved in the cell cycle (GO:007049, false discovery rate <0.001) whereas the most upregulated genes in both Treg and CD4^{LNGFR.FOXP3} came from the Treg upregulated signature (red). The gene names are given beside each group.

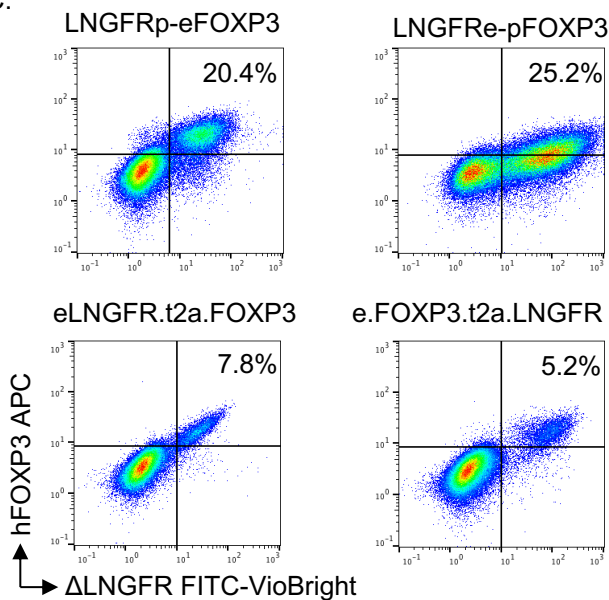
A.



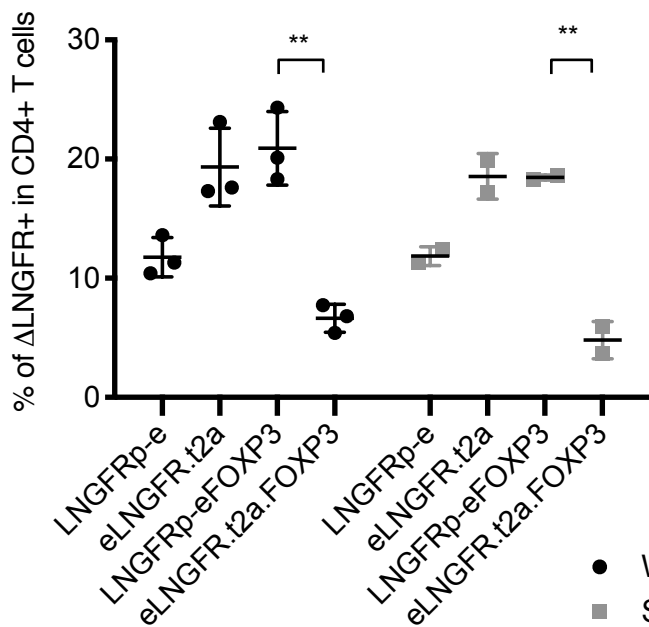
B.

Vectors	Titer (lg/mL)
LNGFRp-e	1.4x10 ⁸
LNGFRp-eFOXP3	1.5x10 ⁹
LNGFRe-p	5.9x10 ⁹
LNGFRe-pFOXP3	4.1x10 ⁹
eLNGFR.t2a	5.9x10 ⁷
eLNGFR.t2a.FOXP3	1.1x10 ⁸
e.t2a.LNGFR	2.3x10 ⁷
eFOXP3.t2a.LNGFR	6.4x10 ⁷

C.



D.



E.

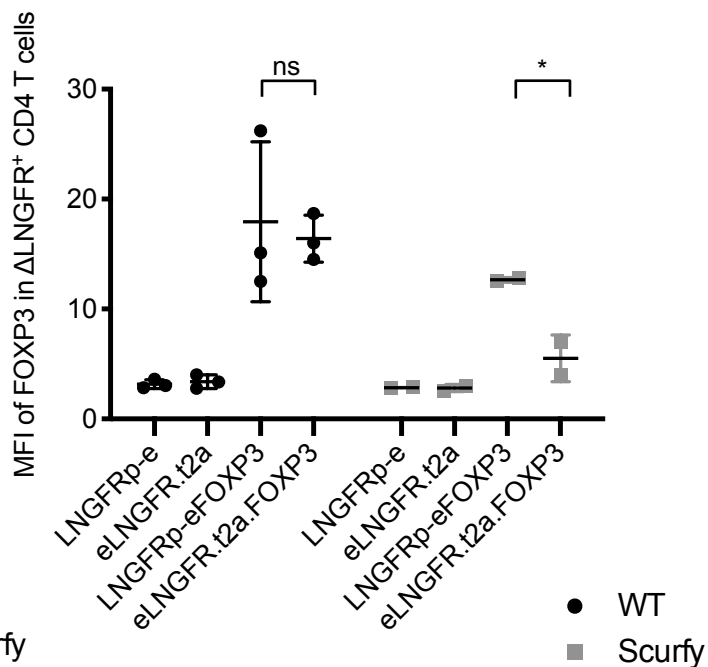
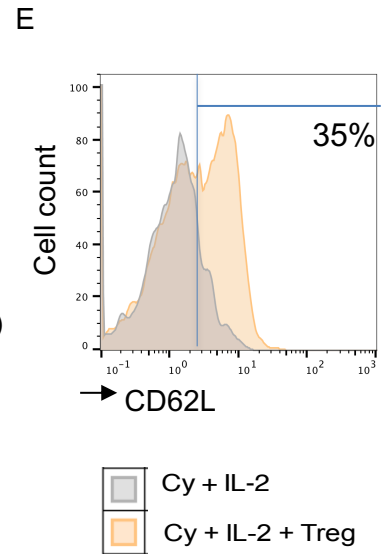
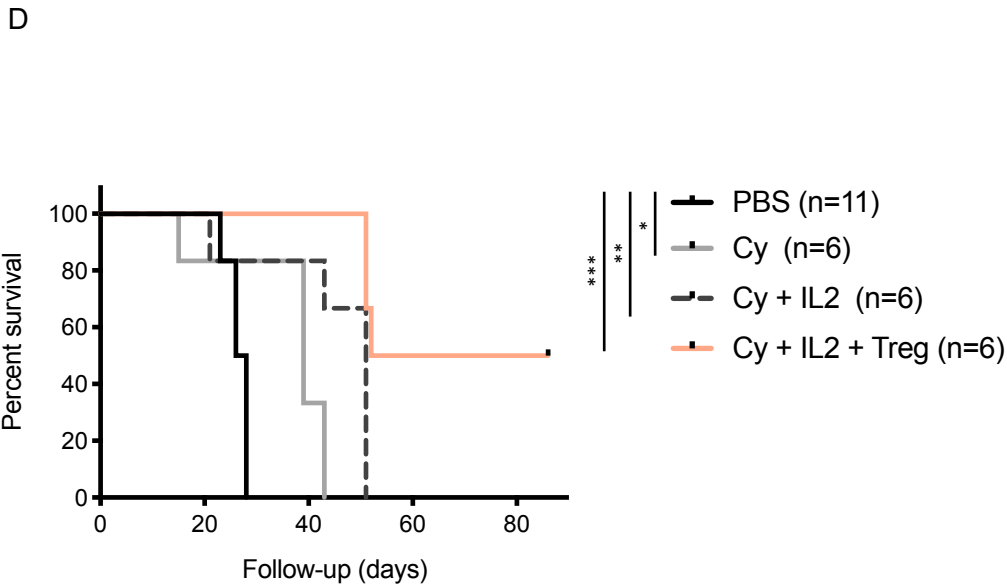
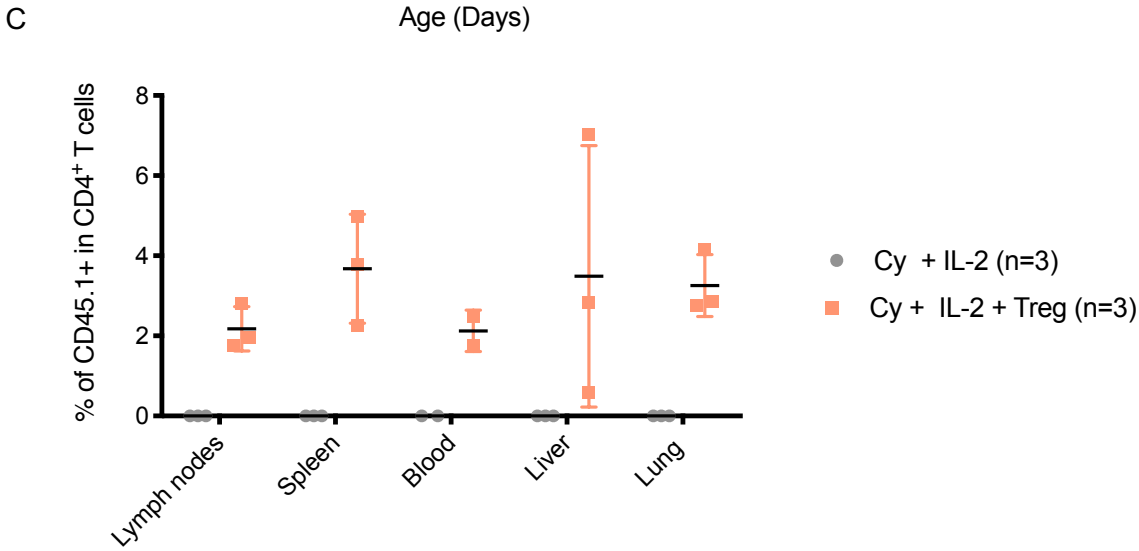
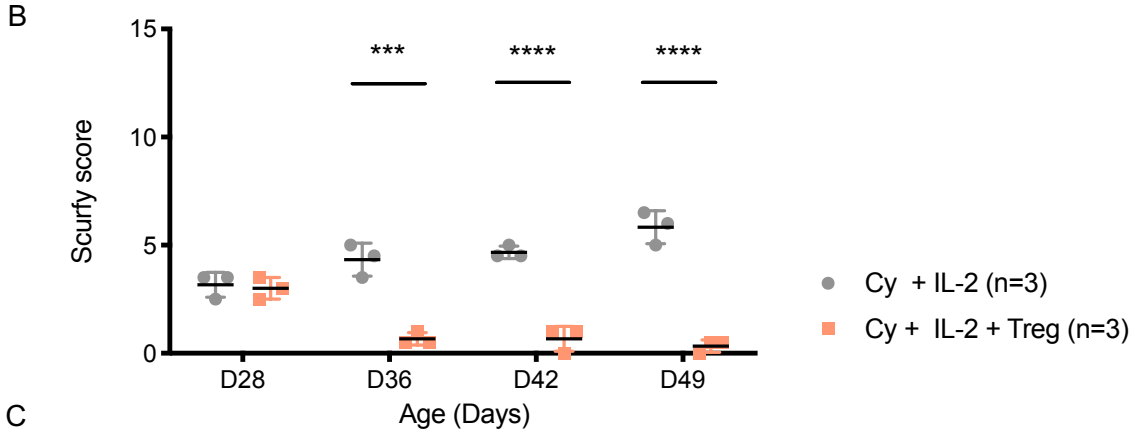
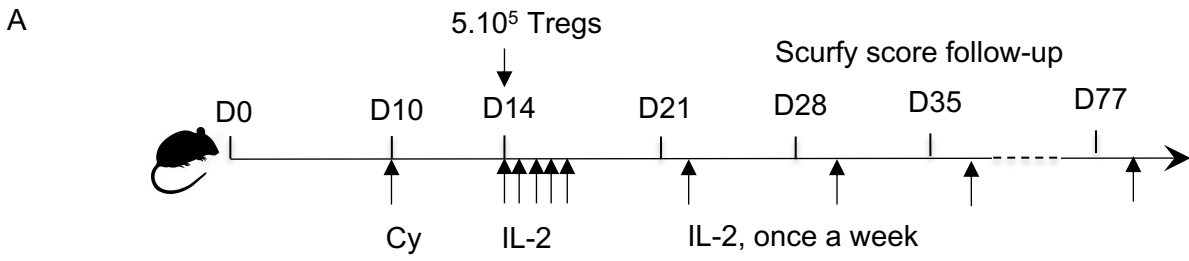
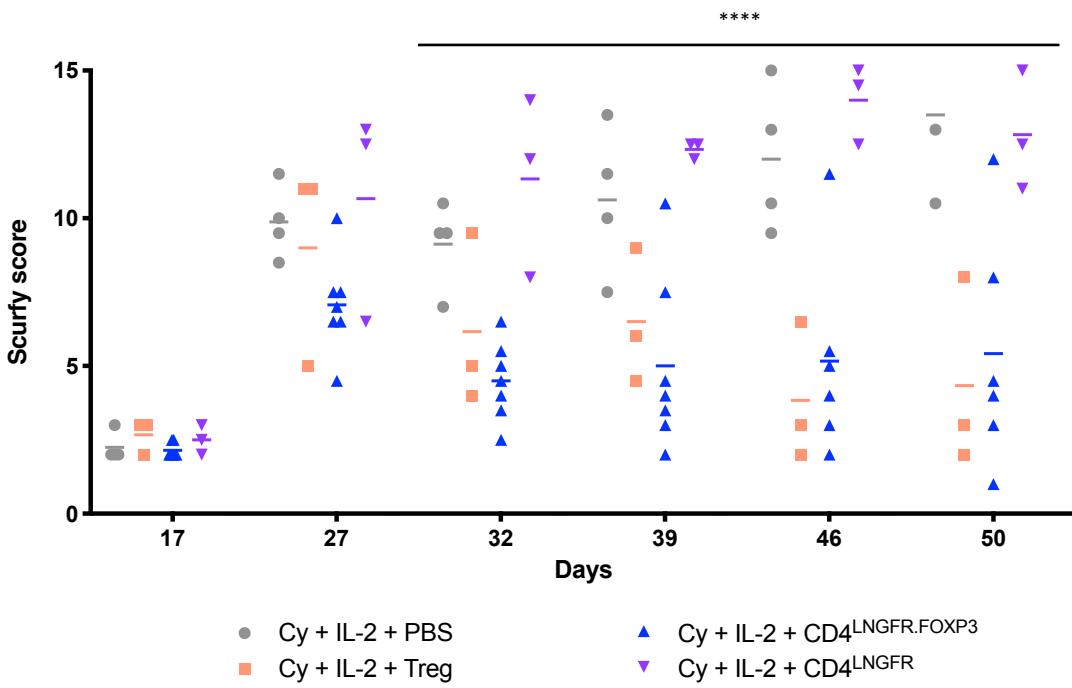
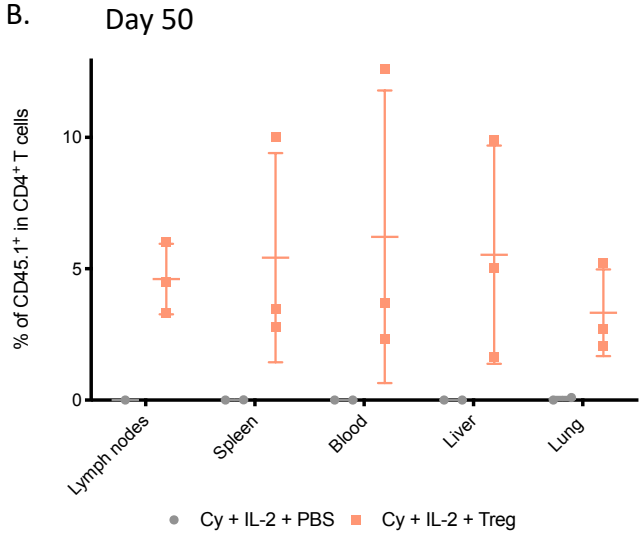


Figure 2

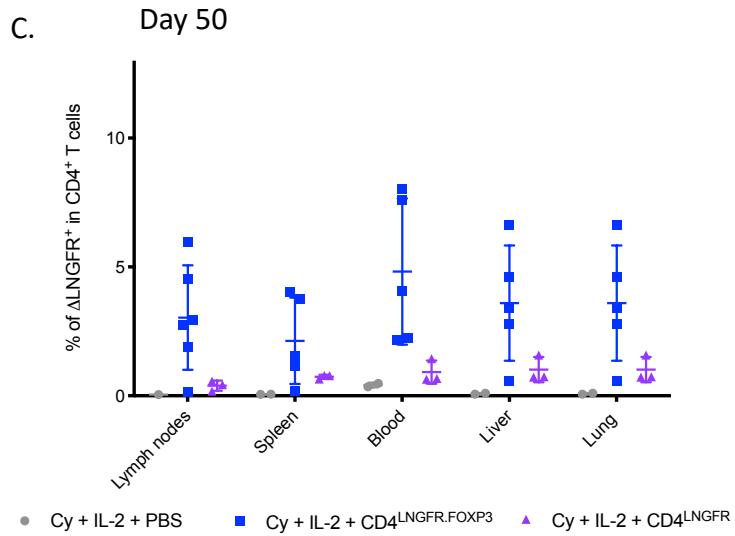
A.



B.



C.



D.

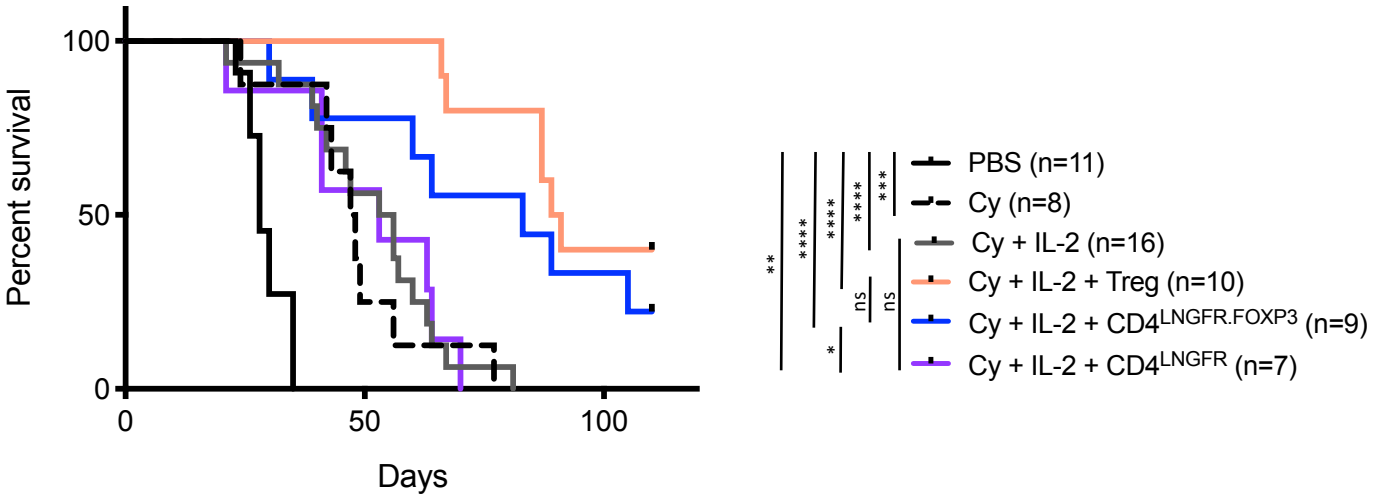


Figure 4

